
Augment then Smooth: Reconciling Differential Privacy with Certified Robustness

Jiapeng Wu
Layer 6 AI
paul@layer6.ai

Atiyeh Ashari Ghomi
Layer 6 AI
atiyeh@layer6.ai

David Glukhov
University of Toronto &
Vector Institute
david.glukhov@mail.utoronto.ca

Jesse C. Cresswell
Layer 6 AI
jesse@layer6.ai

Franziska Boenisch
University of Toronto &
Vector Institute
franziska.boenisch@vectorinstitute.ai

Nicolas Papernot
University of Toronto &
Vector Institute
nicolas.papernot@utoronto.ca

Abstract

Machine learning models are susceptible to a variety of attacks that can erode trust in their deployment. These threats include attacks against the privacy of training data and adversarial examples that jeopardize model accuracy. *Differential privacy* and *randomized smoothing* are effective defenses that provide certifiable guarantees for each of these threats, however, it is not well understood how implementing either defense impacts the other. In this work, we argue that it is possible to achieve both privacy guarantees and certified robustness simultaneously. We provide a framework called DP-CERT for integrating certified robustness through randomized smoothing into differentially private model training. For instance, compared to differentially private stochastic gradient descent on CIFAR10, DP-CERT leads to a 12-fold increase in certified accuracy and a 10-fold increase in the average certified radius at the expense of a drop in accuracy of 1.2%. Through in-depth per-sample metric analysis, we show that the certified radius correlates with the local Lipschitz constant and smoothness of the loss surface. This provides a new way to diagnose when private models will fail to be robust.

1 Introduction

Machine learning (ML) models are becoming increasingly trusted in critical settings despite an incomplete understanding of their properties. This raises questions about the *trustworthiness* of those models, encompassing aspects such as privacy, robustness, and more. Society at large might expect *all* of these properties to hold simultaneously as ML's influence on everyday life expands, but each aspect is challenging enough that scientists and practitioners still mostly grapple with them individually. Relatively little research has been done on the intersectionality of trustworthy ML requirements, since each aspect seems to push us in orthogonal research directions.

We aim to reconcile two key objectives of trustworthy ML, namely *privacy* and *robustness*. Privacy in the context of ML manifests as the requirement that a model does not leak information about the data it was trained on [34], such as revealing whether or not certain data points were included in the training dataset [43] or what characteristics they exhibit [17]. In our study, robustness refers to the requirement that a model's prediction should not change when its test inputs are perturbed, even in the worst case when perturbations are chosen adversarially [2, 45, 19].

The current gold standard for providing privacy guarantees is differential privacy (DP) [13]. In ML, DP produces mathematically rigorous privacy guarantees by limiting the impact of each individual training data point on the final model. This is achieved by clipping per-sample gradients, and adding a well-calibrated amount of noise to all model updates. Clipping serves to bound the *sensitivity* of the training algorithm, while the addition of noise ensures that training will be more likely to output similar models whether any of the individual data points are added to or removed from the training dataset. However, clipping and adding noise can impede the convergence of models [47] and yield decision boundaries that are less smooth [20], negatively impacting robustness [16].

These findings call for integrating robustness measures into private training, yet this remains challenging because most methods to increase robustness use random or adversarial augmentations of training data points, which both conceptually and practically do not align well with DP training. Conceptually, augmenting an input increases the sensitivity of private training to it, and thereby provides additional avenues for information leakage. From a practical viewpoint, since gradients are computed on a per-example basis for DP, augmentations drastically increase the time and memory costs of training.

To bridge the gap between robust and private ML model training, we evaluate the certified robustness of private models and improve it by integrating state-of-the-art techniques [51, 38] with DP training. CR provides probabilistic guarantees that perturbations of a certain magnitude will not change a model’s prediction, regardless of what attack strategy (known or yet unknown) is used to modify the test inputs, and thereby provides future-proof robustness guarantees. A common approach for certifying robustness is *randomized smoothing*, where a classifier’s outputs are averaged over a distribution surrounding the test point [28, 29, 10].

While DP and CR are the most promising standards for providing future-proof privacy and robustness guarantees respectively, their intersection has seen little attention. Recent works [37, 36, 46] propose adding noise or adversarial examples while training to improve CR guarantees, but lack the flexibility to incorporate state-of-the-art methods for non-private training [51, 38], and usually rely on training additional network components. We aim to provide CR guarantees within the standard DP training framework, overcoming several challenges in doing so.

Present Work. We study the possible pitfalls of combining DP and CR in a systematic manner. Through our analysis and ablation studies combining randomized smoothing techniques with DP training, we show that standard DP training of ML models is insufficient to provide strong CR results. We propose DP-CERT, an adaptable framework for integrating CR into standard DP training which effectively incorporates augmentations while managing the additional privacy risks. Compared to private training without augmentations, DP-CERT achieves better robustness on MNIST, Fashion-MNIST, and CIFAR10, and even surpasses the state-of-the-art for robustness on the latter dataset under the same privacy guarantee. Finally, we analyze CR on a per data point basis rather than averaged across test datasets. Using the gradient norm, Hessian spectral norm, and local Lipschitz constant, we find that the certifiable radius has a negative log-linear correlation with these quantities, and compare their distributions across training methods. We conclude with concrete recommendations of best practices for the community to achieve CR and DP simultaneously.

2 Preliminaries

Problem Setup. Consider a classification task with Y classes from a dataset $D = \{(x_i, y_i)\}_{i=1}^n$, where $x_i \in \mathbb{R}^d$ and $y_i \in \{1, \dots, Y\}$ denote the i -th input and label. Let $f_\theta : \mathbb{R}^d \rightarrow \{1, \dots, Y\}$ be a neural network with parameters θ , and F_θ denote the soft classifier which outputs the probability distribution, such that $f_\theta(x) = \arg \max_{y \in \{1, \dots, Y\}} F_\theta(x)_y$, where $F_\theta(x)_y$ denotes the model probability of x being a member of class y .

Differential Privacy and DPSGD. We rely on the rigorous framework of differential privacy (DP) [14] to obtain models with privacy guarantees. DP ensures that a model’s weights at the end of training will be similar in distribution whether or not a particular data point was included in the training set. More formally, let D and D' be two potential training datasets for a model f_θ that differ in only one data point. The training mechanism M guarantees (ϵ, δ) -DP if for all possible sets of outcomes S of the training process, it holds that $\Pr [M(D) \in S] \leq e^\epsilon \Pr [M(D') \in S] + \delta$. The parameter ϵ specifies the privacy level, with smaller ϵ yielding higher privacy, while δ quantifies the probability of the algorithm violating the ϵ privacy guarantee.

To obtain a differentially private variant of stochastic gradient descent (SGD), two modifications need to be made [1]. First, the individual gradients of each data point are clipped to a norm C to limit the sensitivity of the model update caused by each data point. Second, choosing a noise level ρ , noise from $\mathcal{N}(0, \rho^2 C^2 \mathbf{I})$ is added to the aggregated gradients to prevent the changes to the model from revealing too much information about individual data points. We detail the resulting algorithm DPSGD (1) and a more thorough introduction to DP in Appendix A.1.

Certified Robustness. Adversarial examples are a well-studied phenomenon in ML, in which an input to a model is perturbed in ways that do not alter its semantics yet cause the model to misclassify the perturbed input [2, 45, 19]. Formally, for a given labeled datapoint (x, y) and classifier f , an (ℓ_p, ζ) -adversary aims to create an adversarial example x' such that $\|x' - x\|_p < \zeta$ and $f(x') \neq y$. Despite much research, the most common defense against adversarial examples remains adversarial training [19, 58, 39]. While adversarial training improves robustness to known algorithms for finding adversarial examples, it does not guarantee that a model will be robust to all adversarial examples (e.g., those crafted with other attack algorithms). This motivates the development of techniques that can provide certifiable guarantees of robustness to adversarial examples by providing a lower bound r on the distance between a correctly classified input and any adversarial example that may be misclassified [51, 38]. This lower bound is also known as the certification radius.

Randomized Smoothing. One popular approach for establishing certified robustness (CR) guarantees is through probabilistic robustness verification which, with high probability, verifies that no adversarial examples exist within a certain radius of the original input [30]. The most commonly studied method for providing a probabilistic robustness verification is through smoothing a classifier [28, 29, 10] by averaging the class predictions of f using a smoothing distribution μ ,

$$\hat{g}(x) = \arg \max_{c \in [Y]} \int_{\zeta \in \text{supp}(\mu)} \mathbb{I}[f(x + \zeta), c] \mu(\zeta) d\zeta, \quad (1)$$

where $\mathbb{I}[a, b] = 1 \iff a = b$ and 0 otherwise [30]. As computing the integral in Equation (1) is intractable, Monte Carlo sampling is used. We denote the approximation of \hat{g} given by Monte Carlo sampling as g . One can certify at different radii through the choice of smoothing distribution μ . Smoothed classifiers are evaluated in terms of their certified accuracy—the fraction of samples correctly classified when certifying robustness at a given radius r .

A tight ℓ_2 radius was obtained by Cohen et al. [10] when using isotropic Gaussian noise $\mu = \mathcal{N}(x, \sigma^2 \mathbf{I})$, where σ is a hyperparameter that controls a robustness/accuracy tradeoff. In particular, Cohen et al. [10] proved that for any base classifier f , the Gaussian smoothed classifier g is robust around an input x with radius $r = \frac{\sigma}{2}(\Phi^{-1}(p_A) - \Phi^{-1}(p_B))$ where p_A and p_B denote the probabilities of c_A and c_B , the most and second-most probable classes returned by $g(x)$, and Φ^{-1} is the inverse of the standard Gaussian CDF. In fact the exact probabilities p_A and p_B are not needed and one can use lower $\underline{p}_A \leq p_A$ and upper $\overline{p}_B \geq p_B$ bounds instead, approximated by Monte Carlo sampling.

The output of the smoothed classifier $g(x)$ is approximated by aggregating the predictions of a base classifier $f(x + \eta)$ for $\eta \sim \mathcal{N}(0, \sigma^2 \mathbf{I})$. As a high dimensional standard Gaussian assigns almost no mass near its mean 0, ensuring that $g(x)$ is accurate at large certification radii *requires the base classifier f to be accurate on Gaussian perturbed data* [18].

3 Method

Training machine learning models to be both differentially private and certifiably robust poses several challenges. The gradient clipping and noise addition used in DPSGD harms the convergence rate of training [9, 47, 4], while restrictive privacy budgets may further require stopping training prior to convergence. Robustness on the other hand suffers for models that are not converged, as having large gradients at test points makes finding adversarial examples easier [16].

Another challenge surfaces around the use of adversarial training [19] or augmentations of datapoints [10] along with DPSGD. As shown by Cohen et al. [10], data augmentations used for training can enhance a model’s CR, however, it is crucial to ensure that augmented data points do not leak private information about the original. Previous works on the combination of DP and CR have proposed adding noise or adversarial examples during training, but deviate from the standard DPSGD

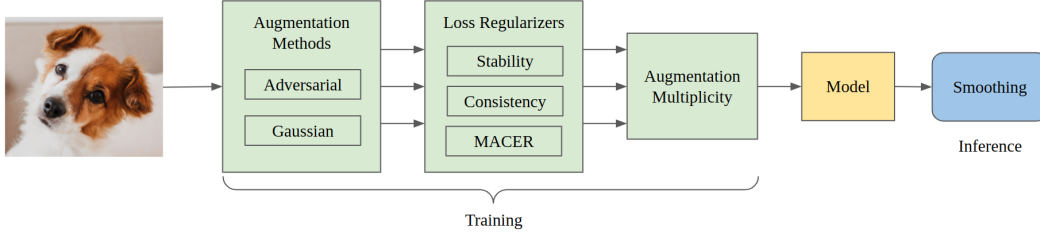


Figure 1: The DP-CERT training framework for providing strong CR guarantees within DPSGD.

template to address the privacy risks [37, 36, 46]. These approaches add trainable model components increasing the overall complexity [37, 46], or lack the flexibility to incorporate the latest advancements in adversarial training methods [36]. For a more detailed description of these related works and comparison to our method, please see Appendix B.

We aim to make CR feasible within the standard training procedure of DPSGD, with state-of-the-art convergence and proper accounting for additional privacy risks by introducing the DP-CERT framework. In this section, we describe DP-CERT, how it effectively manages training with augmented samples while preserving privacy, and how it enables the integration of recent advancements in adversarial training and regularizers to enhance certifiable robustness [40, 29, 56]. Our training framework consists of three stages, summarized in Figure 1: augmentation multiplicity as the foundational stage, plus regularization and adversarial training as two optional stages. After the model is trained, randomized smoothing is used at inference time. We present four instantiations of the framework: DP-Gaussian, DP-SmoothAdv, DP-Stability, and DP-MACER, employing different techniques at each stage.

Augmentation Multiplicity. For each data point (x_i, y_i) , we obtain K augmented data points (x_i^j, y_i) , where $j \in \{1, \dots, K\}$ and x_i^j is the j -th augmented data point. For notational convenience, we use x_i^0 to denote the original data point x_i . As shown by Cohen et al. [10], training with Gaussian data augmentation can enhance a model’s certified robustness. When not using adversarial training, we define $x_i^j = x_i + \eta_j$, $\eta_j \sim \mathcal{N}(0, \sigma^2 \mathbf{I})$ for $j \neq 0$.

An important component of our DP-CERT is how we handle training with augmented data points. We adopt augmentation multiplicity, introduced in [11] and previously unused in studies of CR for DP, which involves averaging the gradients of multiple augmentations of the same training sample before clipping. Since all downstream impact to the model weights from sample x_i is contained in this averaged gradient, clipping it provides a finite sensitivity as required for the Sampled Gaussian Mechanism used in DPSGD [32], and no additional privacy cost is incurred. The model updates can be expressed as follows

$$\theta^{t+1} = \theta^t - \lambda_t \left[\frac{1}{B} \sum_{i \in B_t} \text{clip}_C \left(\frac{1}{K+1} \sum_{j=0}^K \nabla_{\theta^t} L_{\text{CE}}(x_i^j, y_i) \right) + \frac{\rho C}{B} \xi \right]. \quad (2)$$

θ^t denotes the model parameters at iteration t , λ_t is the learning rate, B is the batch size, C is the clipping bound, K is the number of augmentations, ρ is the noise multiplier, $\xi \sim \mathcal{N}(0, \mathbf{I})$, and $\nabla_{\theta^t} L_{\text{CE}}(x_i^j, y_i)$ is the gradient with respect to data point (x_i^j, y_i) . Note that j starts from 0, which means we include the *original samples* along with the augmented ones in model training.

Regularization. We propose adapting stability and consistency regularization to private training in order to minimize the distance between the output probability of the original and augmented examples, hereby improving the robustness to input noise. Stability training [29] adds a smoothed cross-entropy loss as regularization. Inspired by TRADES [57], we instead use the Kullback–Leibler (KL) divergence with a hyperparameter γ controlling the strength of the regularization as:

$$L_{\text{stability}}(x_i, y_i) = \sum_j L_{\text{CE}}(x_i^j, y_i) + \gamma D_{\text{KL}}(F_{\theta}(x_i) || F_{\theta}(x_i^j)). \quad (3)$$

Consistency regularization [25] is a similar technique that instead minimizes the KL divergence between $\hat{F}_{\theta}(x_i)$ and $F_{\theta}(x_i)$, where $\hat{F}_{\theta}(x) = \frac{1}{K} \sum_j F_{\theta}(x_i^j)$ is the average output probability of all

smoothed samples. The loss can be expressed as

$$L_{\text{consistency}}(x_i, y_i) = \sum_j L_{\text{CE}}(x_i^j, y_i) + \gamma D_{\text{KL}}(\hat{F}_\theta(x_i) || F_\theta(x_i^j)). \quad (4)$$

Additionally, we propose integrating MACER [56], an alternative training modification to directly optimize the certified accuracy at larger robustness radii without requiring the costly process of adversarial training. MACER achieves this by decomposing the error of a smoothed classifier into a classification error term and a robustness error term, the latter reflecting whether or not the smoothed classifier was able to certify robustness for a given radius.

Adversarial Training. To achieve better certified accuracy, we incorporate adversarial training by deploying existing attacks to create adversarial examples. Specifically, we integrate SmoothAdv [40] into private training, which, given original data (x, y) , optimizes

$$\arg \max_{\|x' - x\|_2 \leq \epsilon} \left(-\log_{\eta \sim N(0, \sigma^2 \mathbf{I})} \mathbb{E} [F_\theta(x' + \eta)_y] \right), \quad (5)$$

to find an x' ϵ -close to x that maximizes the cross entropy between $g_\theta(x')$ and label y . Using Monte Carlo sampling, Objective (5) can be optimized by iteratively computing the approximate gradient

$$\nabla_{x'} \left(-\log \left(\frac{1}{K} \sum_{j=1}^K F_\theta(x' + \eta_j)_y \right) \right). \quad (6)$$

where $\eta_1, \dots, \eta_K \sim \mathcal{N}(0, \sigma^2 \mathbf{I})$. The approximate gradient is then used to update x' , with the final x' used as examples within augmentation multiplicity.

3.1 Metrics for Interpreting Robustness

To elicit some insights into why certain training methods may produce better-performing models than others, we investigate several per-data point metrics associated with robustness, the *input gradient norm*, *input Hessian spectral norm*, and *local-Lipschitz constant*, and study their relationships with CR. The first two metrics measure the local smoothness of the loss landscape with respect to the input space. Taylor’s approximation can be used to show a direct link between these two metrics and the worst-case change in loss from small input perturbations. Due to this connection, prior works directly regularized them in order to train more robust models [22, 24, 33].

Gradients and Hessians are highly local quantities that are only connected to robustness through Taylor’s approximation at small radii around the input data point. Consequently, they may not be informative at larger radii used to certify robustness. Thus, we also compare models using an empirical estimate of the average local Lipschitz constant of the model’s penultimate layer. By viewing the network as a feature extractor composed with a linear classifier, using the penultimate layer captures the worst-case sensitivity of the feature extractor to perturbations of the data. This metric was initially proposed by Yang et al. [54] to investigate adversarial robustness and is given by

$$\frac{1}{n} \sum_{i=1}^n \max_{x'_i \in B_\infty(x, \zeta)} \frac{\|f(x_i) - f(x'_i)\|_1}{\|x_i - x'_i\|_\infty}, \quad (7)$$

where the maximum is approximated in the same manner as is used for adversarial example generation, typically projected gradient descent (PGD) [31].

4 Experiment Setup

We evaluate the effectiveness of DP-CERT on multiple image classification datasets, including MNIST [27], Fashion-MNIST [53], and CIFAR10 [26]. More detailed data statistics can be found in Appendix C.1. We demonstrate that DP-CERT consistently outperforms the undefended differentially private baselines, and establishes the state of the art for certified l_2 defense under a DP guarantee, via randomized smoothing on CIFAR-10.

4.1 Baselines Methods

Our comparison methods include non-private training (*Regular*) for an accuracy baseline, *DPSGD* to observe the CP properties of standard DP training, and per-sample adaptive clipping (*PSAC*) [52], described in Appendix A.2, which achieves better convergence than DPSGD, all else held equal. For DPSGD and PSAC, we adopt the same settings as Xia et al. [52], who exhibited state-of-the-art performance for DP optimization on various tasks. We additionally compare against prior approaches to integrate CR with DP guarantees, namely TransDenoiser [46], SecureSGD [37] and StoBatch [36] on CIFAR10. We refer to Tang et al. [46] for details of their experimental setting.

4.2 Evaluation Metrics

First, we report the natural accuracy (*Acc*) on the test dataset without randomized smoothing for inference as a measure of convergence. Following previous works, we report the *approximate certified accuracy*, which is the fraction of the test set that can be certified to be robust at radius r using the CERTIFY procedure introduced by [10]. We also include the average certified radius (*ACR*) [56] which represents the average certified radius returned by CERTIFY which serves as an additional metric for better comparison of CR between two models [49, 58]. ACR is calculated as

$$\text{ACR} = \frac{1}{|D_{\text{test}}|} \sum_{(x,y) \in D_{\text{test}}} \text{CR}(f, \sigma, x) \cdot \mathbb{I}[\hat{f}(x), y'], \quad (8)$$

where D_{test} is the test dataset, and CR denotes the certified radius provided by CERTIFY.

4.3 Implementation and Hyperparameters

For all experiments on MNIST and Fashion-MNIST, we train a four-layer CNN model, with the settings use by Tramèr and Boneh [47]. On CIFAR10, we fine-tune a CrossViT-Tiny [8], pretrained on ImageNet1k [12]. We set the learning rate as 0.001 and train the models for 10 epochs. The rest of the hyperparameters are the same as used by [6]. For evaluation, we use CERTIFY with parameters $n = 10,000$, $n_0 = 100$, and $\alpha = 0.001$, following previous work [10, 40]. Our implementations of DP-SmoothAdv, DP-Stability and DP-MACER are adapted from the original codebases [41, 29, 56], and we use the default hyperparameters reported in the original papers. We set the number of augmentations K to 2 for MNIST and Fashion-MNIST, and 1 for CIFAR10, as they bring a better trade-off between certified accuracy and efficiency (see Section 5.2). By default, we compare models using the same privacy guarantee: ($\epsilon = 3.0, \delta = 10^{-5}$).

For each model configuration, we consider three models trained with different noise levels $\sigma \in \{0.25, 0.5, 1.0\}$ for smoothing at training time, and during inference we apply randomized smoothing with the same σ as used in training. The randomized smoothing results for TransDenoiser, SecureSGD and StoBatch are directly copied from Tang et al. [46]. For CIFAR10, TransDenoiser takes a VGG16 model [44] pretrained on a public dataset, then fine-tunes the classifier and the denoisers jointly. For a fair comparison, we use a much smaller network, CrossViT-Tiny [8], in DP-CERT, achieving a similar accuracy on the CIFAR10 test set. For more experimental details, please refer to Appendix C.2. All experiments were conducted on a cluster of 8 Nvidia V100 GPUs. All the training and inference procedures are implemented based on Pytorch v1.13.0 [35] and Opacus v1.3.0 [55], and our code is provided as supplementary material.

5 Experimental Evaluation

5.1 Comparative Study

In Table 1, we compare our baseline methods and DP-CERT instantiations by their natural accuracy, ACR, and certified accuracy for radii greater than 0.25. The best ACR and certified accuracy for each σ are displayed in **bold**, while close runner-ups are underlined. In Figure 2 we plot the certified accuracy as the certified radius is increased on CIFAR10. Similar results for MNIST and Fashion-MNIST are displayed in Figure 7 in Appendix D.1, where we also compare DP-CERT to TransDenoiser, SecureSGD, and StoBatch on CIFAR10 in Figure 8.

Table 1: Comparison of accuracy, ACR and the certified accuracy at radius 0.25 between baselines and instances of the DP-CERT framework on MNIST, Fashion-MNIST and CIFAR10.

σ	Method	MNIST			Fashion-MNIST			CIFAR10		
		Acc	ACR	$r=0.25$	Acc	ACR	$r=0.25$	Acc	ACR	$r=0.25$
0.25	Regular	99.14	0.581	83.6	89.28	0.359	55.5	94.79	0.055	9.5
	DPSGD	98.13	0.606	88.3	85.87	0.343	53.2	89.74	0.023	3.3
	PSAC	98.25	0.608	88.5	86.34	0.320	49.0	89.81	0.020	2.8
	DP-Gaussian	98.13	0.735	95.7	84.76	0.545	<u>75.8</u>	87.61	0.246	41.8
	DP-SmoothAdv	98.08	0.742	96.0	83.97	0.554	75.9	87.89	0.275	44.3
	DP-Stability	97.86	0.738	95.9	84.19	0.551	<u>75.7</u>	88.53	0.246	41.6
	DP-MACER	98.13	0.736	95.6	84.79	0.545	<u>75.8</u>	87.52	0.246	41.7
0.5	Regular	99.14	0.308	31.8	89.28	0.331	34.9	94.79	0.092	9.7
	DPSGD	98.13	0.344	50.0	85.87	0.309	29.8	89.74	0.057	9.8
	PSAC	98.25	0.383	55.9	86.34	0.298	27.5	89.81	0.056	9.8
	DP-Gaussian	97.74	1.246	<u>94.7</u>	82.42	0.879	<u>73.0</u>	87.48	0.288	35.5
	DP-SmoothAdv	97.66	1.258	94.8	82.65	0.894	<u>73.0</u>	87.54	0.263	31.9
	DP-Stability	97.62	1.248	94.6	82.25	0.876	<u>72.7</u>	88.56	0.282	35.4
	DP-MACER	97.75	1.246	<u>94.7</u>	82.50	0.880	73.1	87.36	<u>0.287</u>	35.2
1.0	Regular	99.14	0.257	10.7	89.28	0.342	21.2	94.79	0.079	9.7
	DPSGD	98.13	0.260	10.4	85.87	0.338	13.5	89.74	0.029	5.9
	PSAC	98.25	0.213	20.0	86.34	0.328	11.5	89.81	0.023	4.2
	DP-Gaussian	96.33	1.262	85.6	80.96	<u>1.101</u>	65.4	88.55	0.299	25.4
	DP-SmoothAdv	96.54	1.249	85.0	80.93	1.096	64.7	87.37	0.237	21.0
	DP-Stability	96.48	1.262	84.9	80.66	1.084	65.1	89.09	0.294	25.0
	DP-MACER	96.31	1.262	<u>85.5</u>	80.83	1.102	<u>65.3</u>	88.40	0.255	22.3

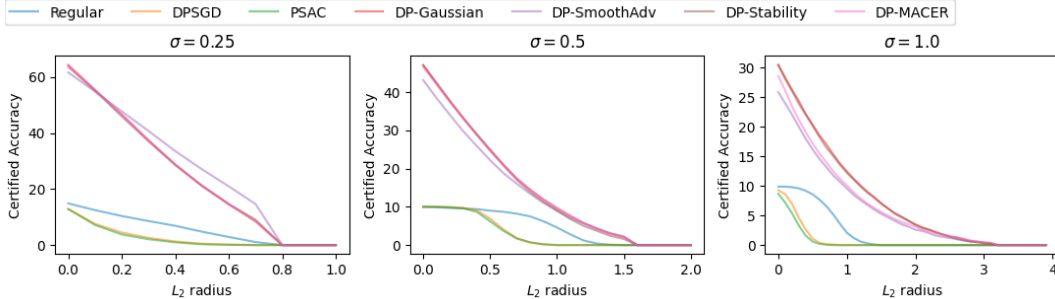


Figure 2: Approximate certified accuracy comparison on CIFAR10.

Discussion. Table 1 and Figure 2 show that all instantiations of DP-CERT significantly outperform the baseline methods in terms of the approximate certified accuracy and ACR. Generally, DP-CERT’s natural accuracy is marginally lower than the PSAC baseline, but its ACR and certified accuracy do not fall off drastically as σ is increased. Hence, there is still a tradeoff between natural accuracy and CR. Our well-converged baselines show that DPSGD training does not always lead to worse CR compared non-private training, which should be contrasted with previous studies on the adversarial robustness of DPSGD [50, 3, 60]. Still, DPSGD alone, even when well-converged, does not provide strong CR, demonstrating the need for DP-CERT’s improvements.

Figure 8 in Appendix D.1 shows that all variants of DP-CERT achieve the state-of-the-art certified accuracy on CIFAR10 with a much smaller pre-trained model compared to [46, 36]. Since we do not rely on an additional denoiser, the inference is much faster with DP-CERT.

Practical recommendation. Contrary to the previous findings in non-private training [40, 56], all variants of DP-CERT have close performance. Because DP-SmoothAdv incurs significantly larger training overhead, we recommend *not* using it in private training. For *training from scratch*, *DP-Gaussian* is recommended since it offers competitive results while being the most straightforward to implement and fastest to train as it does not rely on adversarial examples. For fine-tuning a pre-trained

model, *DP-Stability* is recommended since it has the highest natural accuracy in all variants while offering competitive certified accuracy.

5.2 Studying the Impact of Model Architectures and Augmentations

In this section, as an ablation, we examine the effect of different model variants and hyperparameters. All experiments are run on Fashion-MNIST with $\sigma = 0.5$; results for MNIST and other value of σ are given in Appendix D.2. We combine consistency regularization and PSAC with DP-Gaussian and DP-SmoothAdv to study their effect on certified accuracy and radius. Figure 3 shows that neither of these techniques improves CR. We also train models with different numbers of augmentations and compare their CR. Figure 3 shows that the certified test accuracy is unchanged as the number of augmentations increases, consistent with the observations made by Salman et al. [40]. We emphasize that using no augmentations at all, i.e. plain DPSGD, performs much worse (Table 1). Since fewer augmentations better preserves the natural accuracy and incurs less training overhead, we recommend using a minimal number of augmentations.

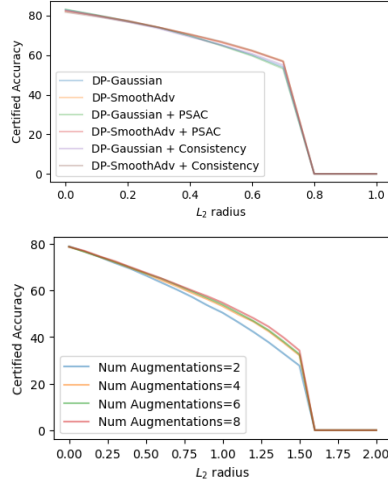


Figure 3: Ablation study for consistency regularization, PSAC, and augmentations.

5.3 Fine-Grained Metric Analysis

Certified accuracy and ACR are both metrics averaged over the test set. However, robustness is inherently sample based, since it examines how resilient the model is against perturbations tailored to individual samples. Therefore, in this section we conduct an in-depth analysis of the distributions of the per-sample metrics introduced in Section 3.1 to provide a deeper understanding of the connections between model properties and CR. We pose two research questions below and answer them using data visualization.

RQ1: How are the training dynamics of different methods reflected in their metric distributions?

We calculate the three metrics for each test set data point, visualize their distribution in histograms, and compare across baselines and our proposed methods. For a detailed analysis we focus on a single setting here – MNIST and $\sigma = 0.5$ in Figure 4. For comparison, we visualize the histograms for different datasets and σ 's in Figures 11 - 15 in Appendix D.3. In Figure 4a, Regular training results in an approximately log-normal distribution for input gradient norms with a mode far greater than for DPSGD variants. Meanwhile, DPSGD is bimodal with some inputs having very large gradient norms which are potentially vulnerable to adversarial examples. This likely arises as a consequence of the clipping employed in the DPSGD training algorithm which effectively down-weights the contributions of hard examples and up-weights the contribution of easy examples [42]. Rarer samples, which would dominate a minibatch gradient for Regular training, are not learned and still have large input gradients at the end of training. PSAC mitigates this issue slightly by explicitly up-weighting hard examples, resulting in a distribution closer to Regular training. DP-Gaussian, on the other hand, shifts the distribution towards lower norm values. Comparing variants of DP-CERT in Figure 4b, DP-Stability has a significantly higher input gradient norm, input Hessian spectral norm and lower local Lipschitz constant than the other three variants. This echoes the observation that TRADES [57] style training results in significantly lower local Lipschitz constants [54].

RQ2: How do the metrics correlate with the certified radius on a per-sample basis? We perform two analyses to visualize the correlation. In Figure 5, we first group examples by their certified radii, then for each group we compute their average metric values and take the logarithm. Across training methods, we see a clear negative correlation between the log metric values and certified radius, which means that examples robust to input noise tend to have lower metric values. However, different methods exhibit different levels of correlation, which is closely related to their average metric value. For example, DP stability on average has a much higher input gradient norm and a much lower local Lipschitz constant than other methods at the same certified radii.

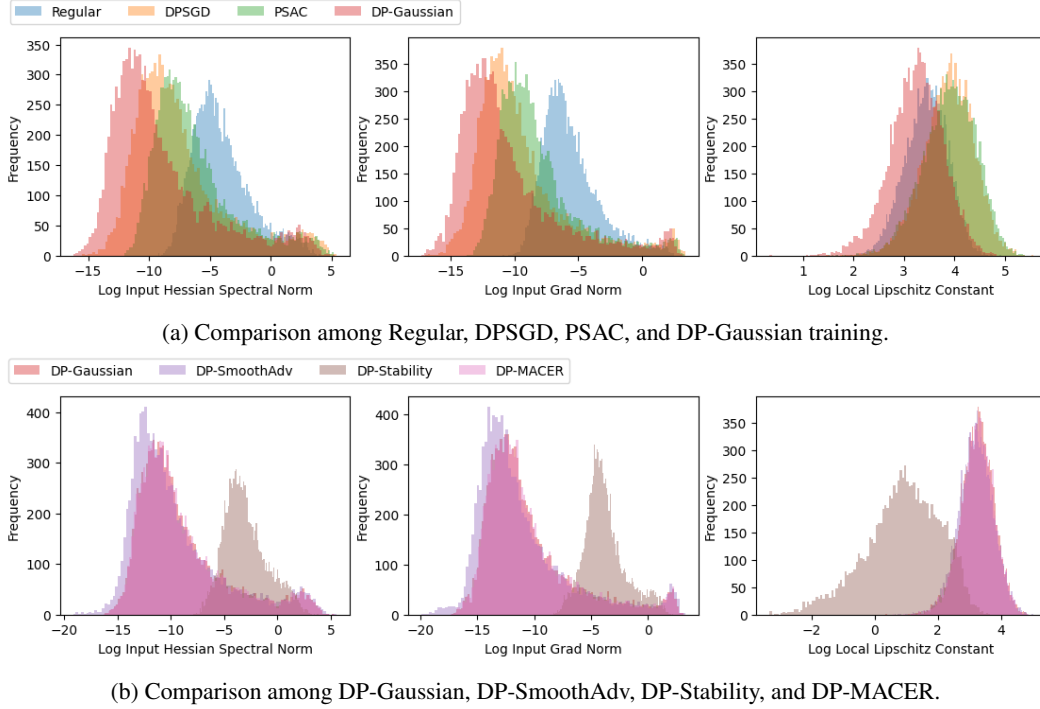


Figure 4: Per-sample metric comparisons on MNIST with $\sigma = 0.5$

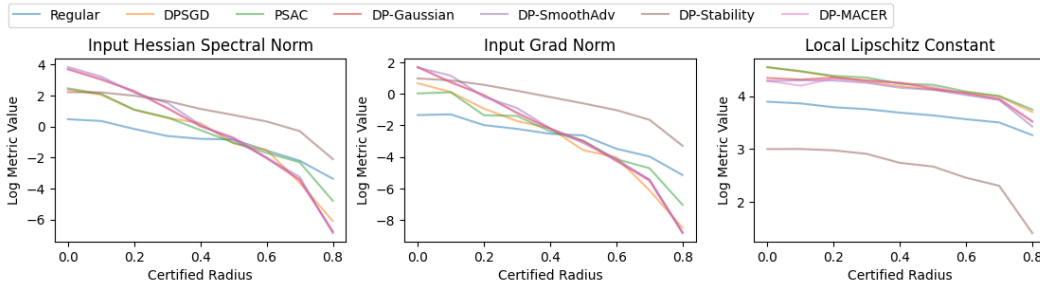
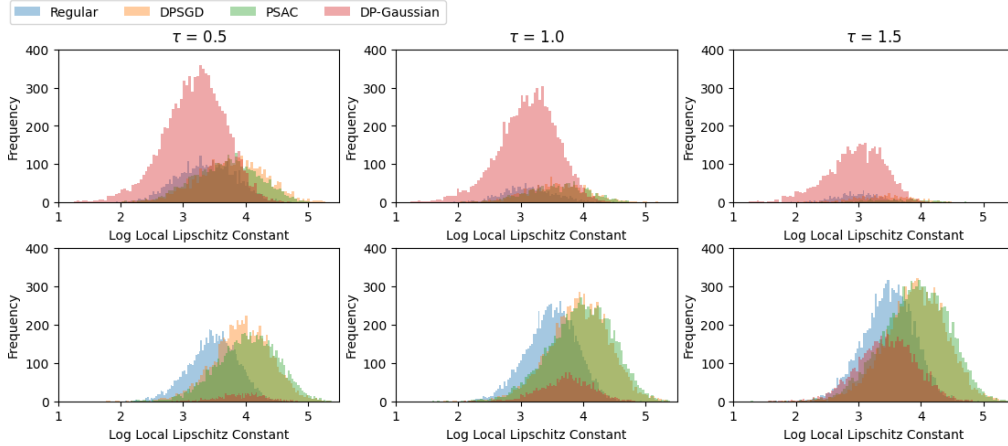
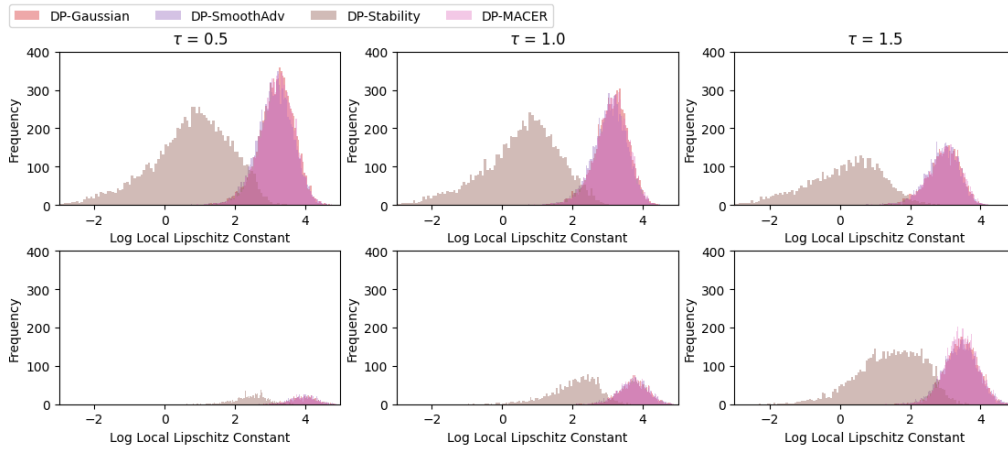


Figure 5: The input Hessian spectral norm (left), input gradient norm (middle), and local Lipschitz constants (right) calculated at different certified radii, on MNIST with $\sigma = 0.5$.

In Figure 6 we select three certified radius thresholds $\tau \in \{0.5, 1.0, 1.5\}$, and separately plot the log of local Lipschitz constants of examples above and below τ on the top and bottom rows of the subfigures respectively. Corresponding plots for the other two metrics are visualized in Figure 18 and 19 in Appendix D.3. We can draw similar conclusions to those from Figure 5. First, the examples with certified radii *below* the threshold have *higher* average local Lipschitz constant. Second, as we increase the threshold τ , more examples with higher local Lipschitz constant end up below the certified radius threshold. Since the local Lipschitz constant is derived using a PGD attack, we anticipate that it naturally correlates with the robustness to adversarial examples. For further comparison, we present the FGSM accuracy on MNIST and Fashion-MNIST under the attack strength in $\{0.0005, 0.01, 0.1, 0.5, 1\}$ in Figure 17 in Appendix D.3. Consistent with the ranking of the average local Lipschitz constant, DP-Stability consistently outperforms other approaches, while DP-Gaussian, DP-SmoothAdv and DP-MACER achieve similar adversarial accuracy over different attack margins.



(a) Per-sample metric comparison among Regular, DPSGD, PSAC, and DP-Gaussian training.



(b) Per-sample metric comparison among DP-Gaussian, DP-SmoothAdv, DP-Stability, and DP-MACER.

Figure 6: Comparing the distribution of local Lipschitz constants among baselines and proposed methods on MNIST under $\sigma = 0.5$. In each subfigure, the examples are classified into ones with certified radius above the threshold τ (top row), and below the threshold (bottom row). We display three thresholds, $\tau \in \{0.5, 1.0, 1.5\}$, and show the logarithmic metric values for all methods.

Summary. In summary, we find that the local Lipschitz constant of test examples has a closer connection to CR than the gradient norm, or Hessian spectral norm for models trained with DP guarantees.

6 Conclusion

We achieve better certified robustness with DPSGD training through augmentations and randomized smoothing, reconciling two crucial objectives for trustworthy ML, namely privacy and robustness. To overcome the theoretical and practical challenges that arise from the combination of both approaches, we rely on state-of-the-art DP training with augmentations that does not incur additional privacy costs. We employ various regularizations, and adversarial training methods to enhance robustness. Our resulting DP-CERT framework is modular and supports multiple combinations of these methods. Through our extensive experimental study, we confirm that DPSGD training alone, even with state-of-the-art convergence, does not provide satisfactory certified robustness. However, introducing a small number of computationally inexpensive augmentations into training, such as adding Gaussian noise, suffices to yield strong privacy protection and certified robustness. By thoroughly analyzing per-sample metrics, we show that the certified radius correlates with the local Lipschitz constant and smoothness of the loss surface; this opens a new path to diagnosing when private models will

fail to be robust. To conclude, our findings yield concrete recommendations for the community to simultaneously achieve CR and DP, providing a valuable contribution towards more trustworthy ML. When training from scratch, Gaussian augmentations (not adversarial) should be used with DPSGD, and randomized smoothing applied at inference time. For fine-tuning pretrained models, adding stability regularization also helps accuracy, and leads to much lower local Lipschitz constants.

Acknowledgments. DG, FB, and NP would like to acknowledge sponsors who support their research with financial and in-kind contributions: CIFAR through the Canada CIFAR AI Chair, NSERC through a Discovery Grant, the Ontario Early Researcher Award, and the Sloan Foundation. Resources used in preparing this research were provided, in part, by the Province of Ontario, the Government of Canada through CIFAR, and companies sponsoring the Vector Institute.

References

- [1] M. Abadi, A. Chu, I. Goodfellow, H. B. McMahan, I. Mironov, K. Talwar, and L. Zhang. Deep learning with differential privacy. In *Proceedings of the 2016 ACM SIGSAC Conference on Computer and Communications Security*. ACM, 2016. doi: 10.1145/2976749.2978318.
- [2] B. Biggio, I. Corona, D. Maiorca, B. Nelson, N. Šrndić, P. Laskov, G. Giacinto, and F. Roli. Evasion attacks against machine learning at test time. In *Machine Learning and Knowledge Discovery in Databases: European Conference*, pages 387–402, 2013.
- [3] F. Boenisch, P. Sperl, and K. Böttinger. Gradient masking and the underestimated robustness threats of differential privacy in deep learning. *arXiv:2105.07985*, 2021.
- [4] Z. Bu, H. Wang, and Q. Long. On the convergence and calibration of deep learning with differential privacy. *arXiv:2106.07830*, 2021.
- [5] Z. Bu, P. Li, and W. Zhao. Practical adversarial training with differential privacy for deep learning. *OpenReview Preprint*, 2022. URL <https://openreview.net/forum?id=1hw-h1C8bch>.
- [6] Z. Bu, J. Mao, and S. Xu. Scalable and efficient training of large convolutional neural networks with differential privacy. In *Advances in Neural Information Processing Systems*, 2022.
- [7] Z. Bu, Y.-X. Wang, S. Zha, and G. Karypis. Automatic clipping: Differentially private deep learning made easier and stronger. *arXiv:2206.07136*, 2022.
- [8] C.-F. R. Chen, Q. Fan, and R. Panda. CrossViT: Cross-Attention Multi-Scale Vision Transformer for Image Classification. In *Proceedings of the IEEE/CVF International Conference on Computer Vision*, pages 357–366, October 2021.
- [9] X. Chen, S. Z. Wu, and M. Hong. Understanding Gradient Clipping in Private SGD: A Geometric Perspective. In *Advances in Neural Information Processing Systems*, 2020.
- [10] J. Cohen, E. Rosenfeld, and Z. Kolter. Certified adversarial robustness via randomized smoothing. In *Proceedings of the 36th International Conference on Machine Learning*, volume 97, pages 1310–1320, 2019.
- [11] S. De, L. Berrada, J. Hayes, S. L. Smith, and B. Balle. Unlocking high-accuracy differentially private image classification through scale. *arXiv:2204.13650*, 2022.
- [12] J. Deng, W. Dong, R. Socher, L.-J. Li, K. Li, and L. Fei-Fei. ImageNet: A large-scale hierarchical image database. In *2009 IEEE Conference on Computer Vision and Pattern Recognition*, pages 248–255, 2009. doi: 10.1109/CVPR.2009.5206848.
- [13] C. Dwork and A. Roth. The Algorithmic Foundations of Differential Privacy. *Found. Trends Theor. Comput. Sci.*, 9(3–4):211–407, Aug. 2014. ISSN 1551-305X. doi: 10.1561/04000000042.
- [14] C. Dwork, F. McSherry, K. Nissim, and A. Smith. Calibrating Noise to Sensitivity in Private Data Analysis. In *Theory of Cryptography*, pages 265–284. Springer Berlin Heidelberg, 2006. ISBN 978-3-540-32732-5.
- [15] M. S. Esipova, A. A. Ghomi, Y. Luo, and J. C. Cresswell. Disparate impact in differential privacy from gradient misalignment. In *The Eleventh International Conference on Learning Representations*, 2023.
- [16] A. Fawzi, S.-M. Moosavi-Dezfooli, P. Frossard, and S. Soatto. Empirical study of the topology and geometry of deep networks. In *Proceedings of the IEEE Conference on Computer Vision and Pattern Recognition*, June 2018.

- [17] M. Fredrikson, S. Jha, and T. Ristenpart. Model inversion attacks that exploit confidence information and basic countermeasures. In *Proceedings of the 22nd ACM SIGSAC Conference on Computer and Communications Security*, page 1322–1333, 2015. doi: 10.1145/2810103.2813677.
- [18] Y. Gao, I. Shumailov, K. Fawaz, and N. Papernot. On the limitations of stochastic pre-processing defenses. In *Advances in Neural Information Processing Systems*, 2022.
- [19] I. J. Goodfellow, J. Shlens, and C. Szegedy. Explaining and harnessing adversarial examples. *arXiv:1412.6572*, 2014.
- [20] J. Hayes, B. Balle, and M. P. Kumar. Learning to be adversarially robust and differentially private. *arXiv:2201.02265*, 2022.
- [21] G. E. Hinton and R. Zemel. Autoencoders, Minimum Description Length and Helmholtz Free Energy. In *Advances in Neural Information Processing Systems*, 1993.
- [22] J. Hoffman, D. A. Roberts, and S. Yaida. Robust Learning with Jacobian Regularization, 2019.
- [23] M. Z. Horváth, M. N. Müller, M. Fischer, and M. Vechev. Boosting randomized smoothing with variance reduced classifiers. *arXiv preprint arXiv:2106.06946*, 2021.
- [24] D. Jakubovitz and R. Giryes. Improving DNN Robustness to Adversarial Attacks using Jacobian Regularization. In *Proceedings of the European Conference on Computer Vision*, 2018.
- [25] J. Jeong and J. Shin. Consistency regularization for certified robustness of smoothed classifiers. In *Advances in Neural Information Processing Systems*, 2020.
- [26] A. Krizhevsky and G. Hinton. Learning multiple layers of features from tiny images. 2009.
- [27] Y. LeCun, C. Cortes, and C. Burges. MNIST handwritten digit database. Available at <http://yann.lecun.com/exdb/mnist>, 2, 2010.
- [28] M. Lecuyer, V. Atlidakis, R. Geambasu, D. Hsu, and S. Jana. Certified robustness to adversarial examples with differential privacy. In *2019 IEEE Symposium on Security and Privacy*, pages 656–672, 2019. doi: 10.1109/SP.2019.00044.
- [29] B. Li, C. Chen, W. Wang, and L. Carin. Certified adversarial robustness with additive noise. In *Advances in Neural Information Processing Systems*, 2019.
- [30] L. Li, T. Xie, and B. Li. SoK: Certified Robustness for Deep Neural Networks. In *2023 IEEE Symposium on Security and Privacy*, pages 94–115, 2023. doi: 10.1109/SP46215.2023.00006.
- [31] A. Madry, A. Makelov, L. Schmidt, D. Tsipras, and A. Vladu. Towards deep learning models resistant to adversarial attacks. In *International Conference on Learning Representations*, 2018.
- [32] I. Mironov, K. Talwar, and L. Zhang. Rényi Differential Privacy of the Sampled Gaussian Mechanism. *arXiv:1908.10530*, 2019.
- [33] S.-M. Moosavi-Dezfooli, A. Fawzi, J. Uesato, and P. Frossard. Robustness via curvature regularization, and vice versa. In *Proceedings of the IEEE/CVF Conference on Computer Vision and Pattern Recognition*, June 2019.
- [34] N. Papernot, P. McDaniel, A. Sinha, and M. P. Wellman. SoK: Security and Privacy in Machine Learning. In *2018 IEEE European Symposium on Security and Privacy*, pages 399–414, 2018. doi: 10.1109/EuroSP.2018.00035.
- [35] A. Paszke, S. Gross, F. Massa, A. Lerer, J. Bradbury, G. Chanan, T. Killeen, Z. Lin, N. Gimelshein, L. Antiga, A. Desmaison, A. Kopf, E. Yang, Z. DeVito, M. Raison, A. Tejani, S. Chilamkurthy, B. Steiner, L. Fang, J. Bai, and S. Chintala. PyTorch: An Imperative Style, High-Performance Deep Learning Library. In *Advances in Neural Information Processing Systems*, volume 32, 2019.
- [36] H. Phan, M. T. Thai, H. Hu, R. Jin, T. Sun, and D. Dou. Scalable differential privacy with certified robustness in adversarial learning. In *Proceedings of the 37th International Conference on Machine Learning*, volume 119, pages 7683–7694, 2020.
- [37] N. Phan, M. N. Vu, Y. Liu, R. Jin, D. Dou, X. Wu, and M. T. Thai. Heterogeneous gaussian mechanism: Preserving differential privacy in deep learning with provable robustness. In *Proceedings of the Twenty-Eighth International Joint Conference on Artificial Intelligence, IJCAI-19*, 2019. doi: 10.24963/ijcai.2019/660.

- [38] A. Raghunathan, J. Steinhardt, and P. Liang. Certified defenses against adversarial examples. In *International Conference on Learning Representations*, 2018.
- [39] S.-A. Rebuffi, S. Gowal, D. A. Calian, F. Stimberg, O. Wiles, and T. A. Mann. Data augmentation can improve robustness. In *Advances in Neural Information Processing Systems*, volume 34, 2021.
- [40] H. Salman, J. Li, I. Razenshteyn, P. Zhang, H. Zhang, S. Bubeck, and G. Yang. Provably robust deep learning via adversarially trained smoothed classifiers. In *Advances in Neural Information Processing Systems*, 2019.
- [41] H. Salman, M. Sun, G. Yang, A. Kapoor, and J. Z. Kolter. Denoised smoothing: A provable defense for pretrained classifiers. In *Advances in Neural Information Processing Systems*, 2020.
- [42] A. S. Shamsabadi and N. Papernot. Losing less: A loss for differentially private deep learning. *OpenReview Preprint*, 2022. URL <https://openreview.net/forum?id=u7PVCewFya>.
- [43] R. Shokri, M. Stronati, C. Song, and V. Shmatikov. Membership inference attacks against machine learning models. In *2017 IEEE Symposium on Security and Privacy*, pages 3–18, 2017. doi: 10.1109/SP.2017.41.
- [44] K. Simonyan and A. Zisserman. Very deep convolutional networks for large-scale image recognition. *arXiv:1409.1556*, 2014.
- [45] C. Szegedy, W. Zaremba, I. Sutskever, J. Bruna, D. Erhan, I. Goodfellow, and R. Fergus. Intriguing properties of neural networks. *arXiv:1312.6199*, 2013.
- [46] P. Tang, W. Wang, X. Gu, J. Lou, L. Xiong, and M. Li. Two Birds, One Stone: Achieving both Differential Privacy and Certified Robustness for Pre-trained Classifiers via Input Perturbation. *OpenReview preprint*, 2022. URL <https://openreview.net/forum?id=keQjAwuC7j->.
- [47] F. Tramèr and D. Boneh. Differentially private learning needs better features (or much more data). In *International Conference on Learning Representations*, 2021.
- [48] F. Tramèr, A. Kurakin, N. Papernot, I. Goodfellow, D. Boneh, and P. McDaniel. Ensemble adversarial training: Attacks and defenses. *arXiv:1705.07204*, 2017.
- [49] D. Tsipras, S. Santurkar, L. Engstrom, A. Turner, and A. Madry. Robustness may be at odds with accuracy. In *International Conference on Learning Representations*, 2019.
- [50] N. Tursynbek, A. Petiushko, and I. Oseledets. Robustness threats of differential privacy. *arXiv:2012.07828*, 2021.
- [51] E. Wong and Z. Kolter. Provable defenses against adversarial examples via the convex outer adversarial polytope. In *Proceedings of the 35th International Conference on Machine Learning*, 2018.
- [52] T. Xia, S. Shen, S. Yao, X. Fu, K. Xu, X. Xu, X. Fu, and W. Wang. Differentially private learning with per-sample adaptive clipping. *arXiv:2212.00328*, 2022.
- [53] H. Xiao, K. Rasul, and R. Vollgraf. Fashion-MNIST: A novel image dataset for benchmarking machine learning algorithms. *arXiv:1708.07747*, 2017.
- [54] Y.-Y. Yang, C. Rashtchian, H. Zhang, R. R. Salakhutdinov, and K. Chaudhuri. A closer look at accuracy vs. robustness. In *Advances in Neural Information Processing Systems*, 2020.
- [55] A. Yousefpour, I. Shilov, A. Sablayrolles, D. Testuggine, K. Prasad, M. Malek, J. Nguyen, S. Ghosh, A. Bharadwaj, J. Zhao, G. Cormode, and I. Mironov. Opacus: User-friendly differential privacy library in PyTorch. *arXiv:2109.12298*, 2021.
- [56] R. Zhai, C. Dan, D. He, H. Zhang, B. Gong, P. Ravikumar, C.-J. Hsieh, and L. Wang. MACER: Attack-free and Scalable Robust Training via Maximizing Certified Radius. In *International Conference on Learning Representations*, 2020.
- [57] H. Zhang, Y. Yu, J. Jiao, E. Xing, L. El Ghaoui, and M. Jordan. Theoretically principled trade-off between robustness and accuracy. In *International conference on machine learning*, pages 7472–7482. PMLR, 2019.
- [58] H. Zhang, Y. Yu, J. Jiao, E. Xing, L. E. Ghaoui, and M. Jordan. Theoretically principled trade-off between robustness and accuracy. In *Proceedings of the 36th International Conference on Machine Learning*, pages 7472–7482, 2019.

- [59] J. Zhang, Z. Zhang, X. Xiao, Y. Yang, and M. Winslett. Functional mechanism: regression analysis under differential privacy. *arXiv preprint arXiv:1208.0219*, 2012.
- [60] Y. Zhang and Z. Bu. Differentially private optimizers can learn adversarially robust models. *arXiv:2211.08942*, 2022.

A Differential Privacy Background

A.1 Differential Privacy and DPSGD

Differential Privacy (DP) [14] is a formal framework that aims to provide mathematical guarantees on the privacy of individual data points in a dataset, while allowing one to learn properties over the entire dataset. More formally a randomized mechanism M fulfills (ϵ, δ) -DP if

$$\Pr [M(D) \in S] \leq e^\epsilon \Pr [M(D') \in S] + \delta, \quad (9)$$

where D and D' are neighboring datasets (i.e. datasets differing in only one data point), S is the set of output values of M , and ϵ and δ are privacy parameters.

ϵ indicates the level of obtained privacy, with a smaller value of ϵ indicating a stronger privacy guarantee. δ accounts for the probability that the algorithm can violate the privacy guarantee, i.e., not stay within the specified ϵ . A larger value of δ increases the chance of privacy leakage.

The most popular algorithm for implementing DP guarantees in ML is differentially private stochastic gradient descent (DPSGD) [1]. It extends the standard SGD algorithm with two additional steps, namely gradient clipping and noise addition. While the former bounds the sensitivity of the model update, the latter implements the privacy guarantee by preventing the gradients from revealing too much information about individual data points. More formally, let θ_t denote the model parameters at training iteration t . At each iteration t , DPSGD computes the gradient of the loss function with respect to θ_t at an individual data point x as $\nabla_{\theta} L(\theta_t, x)$. The data point's gradient is then clipped to a maximum norm C using the operation $\text{clip}(\nabla_{\theta} L(\theta_t, x), C)$, which replaces the gradient with a vector of the same direction but smaller magnitude if its norm exceeds C . The clipped gradient from all datapoints in a batch are aggregated, then perturbed by adding random noise from $\mathcal{N}(0, \rho^2 C^2 \mathbf{I})$, where ρ is the noise scale parameter. We detail DPSGD in Algorithm 1.

Algorithm 1 Standard DPSGD, adapted from [1].

Require: Private training set $D = \{(x_i, y_i) \mid i \in [N_{\text{prv}}]\}$, loss function $L(\theta_t, x)$, Parameters: learning rate η_t , noise scale ρ , group size B , gradient norm bound C .

- 1: **Initialize** θ_0 randomly
 - 2: **for** $t \in [T]$ **do**
 - 3: Sample mini-batch B_t with sampling probability B/N_{prv} {Poisson sampling}
 - 4: For each $i \in B_t$, compute $\mathbf{g}_t(x_i) \leftarrow \nabla_{\theta} L(\theta_t, x_i)$ {Compute per-sample gradients}
 - 5: $\tilde{\mathbf{g}}_t(x_i) \leftarrow \mathbf{g}_t(x_i) / \max\left(1, \frac{\|\mathbf{g}_t(x_i)\|_2}{C}\right)$ {Clip gradients}
 - 6: $\tilde{\mathbf{g}}_t \leftarrow \frac{1}{|B_t|} \left(\sum_i \tilde{\mathbf{g}}_t(x_i) + \mathcal{N}(0, \rho^2 C^2 \mathbf{I})\right)$ {Add noise to aggregated gradient}
 - 7: $\theta_{t+1} \leftarrow \theta_t - \eta_t \tilde{\mathbf{g}}_t$ {Gradient Descent}
 - 8: **end for**
 - 9: **Output** θ_T and compute the overall privacy cost (ϵ, δ) using a privacy accounting method.
-

A.2 DP-PSAC

We used DP-PSAC [52] in addition to DPSGD to ensure differential privacy while training. Per-sample adaptive clipping (PSAC) is one of a number of approaches that tries to reduce the bias from per-example clipping [4, 7, 15], and was motivated for maximizing the signal to noise ratio of gradient updates. It has shown the best performance on several datasets including MNIST, FashionMNIST and CIFAR10. To compare with DPSGD, we incorporated DP-PSAC into our experiments.

DP-PSAC is similar to DPSGD, with the exception that it employs a different clipping method,

$$\text{clip}_{C,r}(g_{i,t}) = C \cdot g_{i,t} / \left(\|g_{i,t}\| + \frac{r}{\|g_{i,t}\| + r} \right). \quad (10)$$

Where $g_{i,t}$ denotes the loss gradient for the i th sample at iteration t . The motivation of this clipping method is that per-example gradients with small norms come from data points on which the model has already converged, and these gradients are often orthogonal to mini-batch gradients. Hence, small norm gradients should not have disproportionately large contributions to the batch gradient as when using per-sample normalization methods [7]. Compared to such approaches, PSAC reduces the influence of small norm gradients.

B Additional Background and Related Work

B.1 Randomized Smoothing

Previous works have tackled improving the certified robustness of randomized smoothing methods in a variety of ways. The dominant approach for doing so involves modifications to training the base classifier so as to increase robustness and accuracy under Gaussian perturbations. The simplest approach involves adding noise to inputs during training [10], while other works utilize regularization [56, 29, 25], ensembling [23], and adversarial training [40]. While these modifications have been independently studied in the context of improving the certified accuracy of randomized smoothing classifiers, we are the first work integrating these methods with private training through augmentation multiplicity. We provide additional information on two of these training modification methods mentioned in Section 3.

B.1.1 SmoothAdv

One of the most effective methods for improving the performance of randomized smoothing classifiers utilizes adversarial training of the classifier. The method, SmoothAdv proposed in [40], was motivated by the idea that to improve certified accuracy at a larger certification radius one needs a classifier that is more robust to local perturbations, and the best known method of achieving that is through adversarial training.

Given a soft classifier $F : \mathbb{R}^d \rightarrow P(Y)$ where $P(Y)$ is the set of probability distributions over Y , its smoothed soft classifier G is defined as:

$$G(x) = (F * \mathcal{N}(0, \sigma^2 I))(x) = \mathbb{E}_{\delta \sim \mathcal{N}(0, \sigma^2 I)}[F(x + \delta)]. \quad (11)$$

The goal of SmoothAdv is to find a point \hat{x} that maximizes the loss of G in an l_2 ball around x for the cross entropy loss. They use a projected gradient descent variant to approximately find \hat{x} , and define $J(x') = l_{\text{CE}}(G(x'), y)$ to compute

$$\Delta_{x'} J(x') = \Delta_{x'} \left(-\log \mathbb{E}_{\delta \sim \mathcal{N}(0, \sigma^2 I)}[F(x' + \delta)_y] \right). \quad (12)$$

Since the expectation in Equation 12 is difficult to compute exactly, a Monte Carlo approximation is used by sampling noise $\delta_1, \dots, \delta_m \sim \mathcal{N}(0, \sigma^2 I)$ to approximately compute $\Delta_{x'} J(x')$,

$$\Delta_{x'} J(x') \approx \Delta_{x'} \left(-\log \left(\frac{1}{m} \sum_{i=1}^m [F(x' + \delta_i)_y] \right) \right). \quad (13)$$

Finally, x' is updated by taking a step in the direction of $\Delta_{x'} J(x')$, and the final x' is used to train the classifier.

B.1.2 MACER

Similar to the Stability training method from Equation 3, MACER [56] also modifies the loss for optimization so that the final model has higher certified accuracy at a larger certified radius. In contrast to SmoothAdv, regularizing the model to be more robust in this sense does not require generation of adversarial examples and instead can be optimized directly. The method achieves this by decomposing the error of the smoothed classifier into a classification error term and a robustness error term. The former captures the error from the smoothed classifier misclassifying a given datapoint and the latter captures the error of a certified radius being too small.

Robustness error, much like hard label classification error, cannot be optimized directly. To address this, MACER proposes a surrogate loss to minimize the robustness error term—a hinge loss on the data (x, y) for which $g_\theta(x) = y$,

$$\max\{0, \gamma - (\Phi^{-1}(\hat{f}_\theta(x)_y) - \Phi^{-1}(\hat{f}_\theta(x)_{\hat{y} \neq y}))\}, \quad (14)$$

where $\hat{f}_\theta(x)$ denotes the average of softmax probabilities on Gaussian perturbations of x , $\hat{f}_\theta(x)_y$ denotes the softmax probability $\hat{f}_\theta(x)$ assigned to the true class y , and $\hat{f}_\theta(x)_{\hat{y} \neq y}$ denotes the maximum softmax probability for a class that isn't the true class. This loss term is added to cross entropy of loss from the soft smoothed classifier as a regularization term.

B.2 DPSGD and Robustness

The adversarial robustness of differentially private models has been studied in several prior works. Tursynbek et al. [50] demonstrated that models trained with DPSGD are sometimes more vulnerable to input perturbations. Boenisch et al. [3] further consolidate this claim with more experiments, and showed that improper choices of hyperparameters can lead to gradient masking. Zhang and Bu [60] find that the success of adversarially training robust models with DPSGD depends greatly on choices of hyperparameters, namely smaller clipping thresholds and learning rates, differing from those that produce the most accurate models. Furthermore, they found that pretraining models helps further mitigate the privacy-robustness-accuracy tradeoff. These works reveal interesting adversarial robustness characteristics of DP models, however, they do not endeavor to *improve* the robustness of DP models.

DP-ADV [5] proposes combining adversarial training with DPSGD. They achieve this by replacing the original example with an adversarially crafted example, obtained with a FGSM or PGD attack. Their work is orthogonal to ours in that they focus on the robustness to adversarial attacks, whereas we focus on certified robustness. Additionally, they do not perform any data augmentation, which has been shown to be effective against adversarial attacks [39].

There are a few prior works that have studied certified robustness with differential privacy guarantees. Phan et al. [37] first introduced a framework called Secure-SGD, which aims to achieve both certified robustness and differential privacy simultaneously. They use a PixelDP approach, proposed by Lecuyer et al. [28], to attain certified robustness and introduced the Heterogeneous Gaussian Mechanism, which involves adding heterogeneous Gaussian noise instead of element-wise Gaussian noise to the gradient. Another work [36] introduced the StoBatch algorithm to guarantee DP and certified robustness. First, it employs an Autoencoder (AE) [21] and a functional mechanism (objective perturbation [59]) to reconstruct input examples while preserving DP. Subsequently, this reconstructed data is used to train a deep neural network. They implement adversarial training [48] to achieve both robustness and DP for the neural network. Tang et al. [46] propose transforming input gradients with perturbation during training, and introduced the Multivariate Gaussian Mechanism. This mechanism allows them to achieve the same DP guarantee with less noise added to the gradient. They follow the architecture of denoised smoothing, adding differentially private noise to a pre-trained classifier.

Compared with the existing work, DP-CERT 1) presents a simple and effective augmented training scheme, allowing practitioners to introduce different adversarial training techniques through noising, regularization, and adversarially crafted examples, 2) doesn't rely on a denoiser at the inference time, reducing inference latency, and 3) can be used for training both randomly initialized or pre-trained networks.

C Experimental Details

C.1 Dataset Statistics

We conduct experiments on MNIST, Fashion-MNIST and CIFAR10. The MNIST database of handwritten digits has a training set of 60,000 examples, and a test set of 10,000 examples, as does Fashion-MNIST. Each example in MNIST and Fashion-MNIST is a 28×28 grayscale image, associated with one label from 10 classes.

The CIFAR-10 dataset consists of 60,000 RGB images from 10 classes, with 6,000 images per class. There are 50,000 training images and 10,000 test images of size $32 \times 32 \times 3$.

C.2 Code and Implementation

Our code will be released upon publication. We give credit to the original repository for the implementation of SmoothAdv, MACER, stability, and consistency regularization.¹ For CERTIFY² and local Lipschitz constant³ evaluations, we use the code provided by the original authors.

¹<https://github.com/jh-jeong/smoothing-consistency>

²<https://github.com/locuslab/smoothing>

³<https://github.com/yangarbitrator/robust-local-lipschitz>

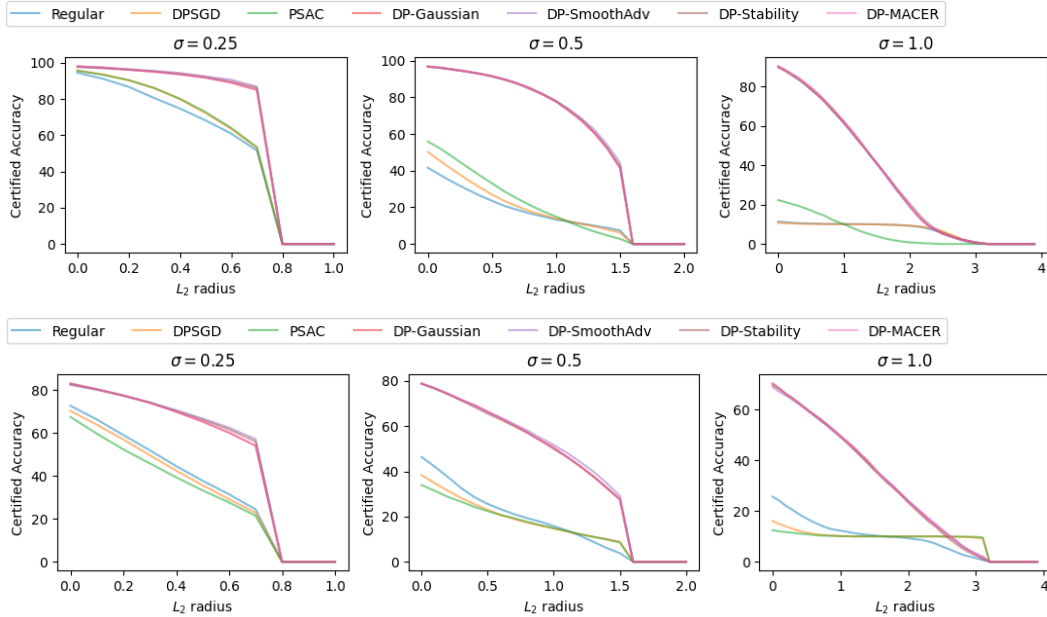


Figure 7: Approximate certified accuracy comparison on MNIST (top), and Fashion-MNIST (bottom).

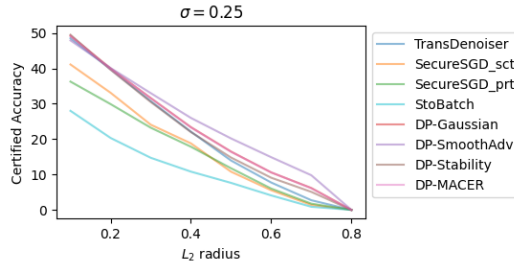


Figure 8: Approximate certified accuracy comparison on CIFAR10. Baseline results are from [46].

D Additional Results

D.1 Additional Comparative Study

Figure 7 shows the approximate certified accuracy as the certified radius is increased on MNIST and Fashion-MNIST, corresponding to Table 1 in the main text, for different values of the noise σ used during training. All variants of DP-CERT greatly outperform the baseline methods which do not specifically encourage robustness. Similar plots for CIFAR10 were shown in Figure 2 in the main text. We also compare implementations of DP-CERT to the prior approaches TransDenoiser, SecureSGD, and StoBatch on CIFAR10 in Figure 8. All variants of DP-CERT achieve state-of-the-art certified accuracy on CIFAR10 for differentially private models, with a much smaller pre-trained model compared to [46].

D.2 Additional Ablation Study

To extend Figure 3 from the main text, we show the complete ablation study results in Figures 9 and 10 on MNIST and Fashion-MNIST under $\sigma \in \{0.25, 0.5, 1.0\}$. Figure 9 shows the effects of adding consistency regularization, or changing the DP clipping method to PSAC. Neither approach makes significant changes to the certified accuracy. Figure 10 shows the effects of changing the multiplicity of augmentations. Again, there is little difference in certified accuracy when using more than two augmentations, so we advocate using the smallest amount which is least expensive computationally. We emphasize that using *no* augmentations is significantly worse than using two or more – the case without augmentations is simply DPSGD which was compared in Table 1 and Figures 2 and 7. One of our main conclusions is that adding a small number of Gaussian augmentations to DPSGD is sufficient to greatly improve certified robustness.

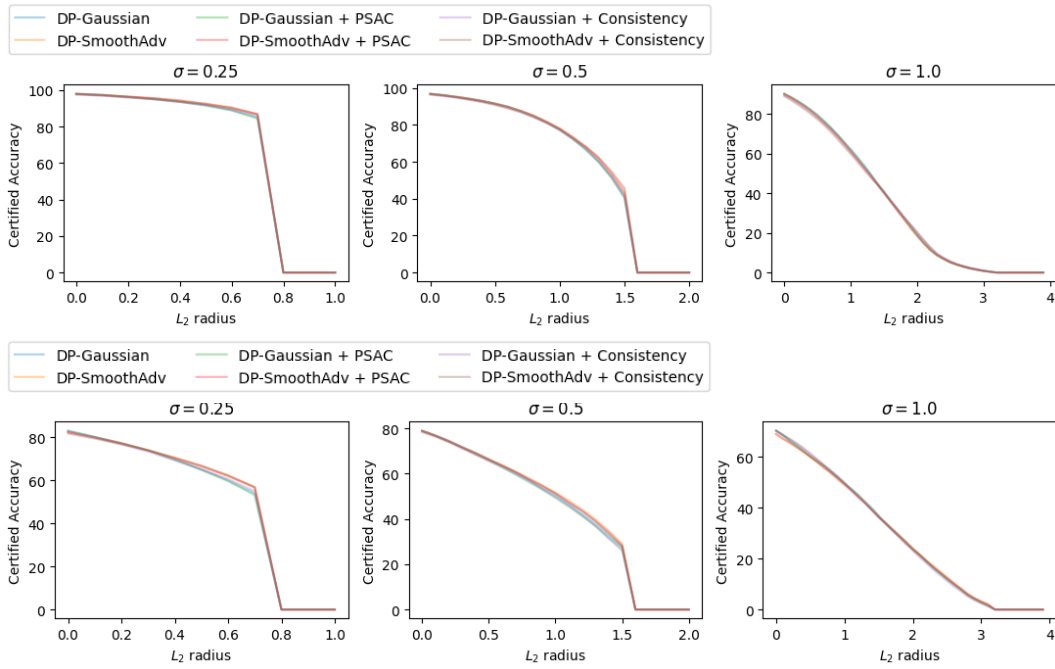


Figure 9: Certified accuracy of DP-Gaussian and DP-SmoothAdv combined with consistency regularization and PSAC on MNIST (top) and Fashion-MNIST (bottom).

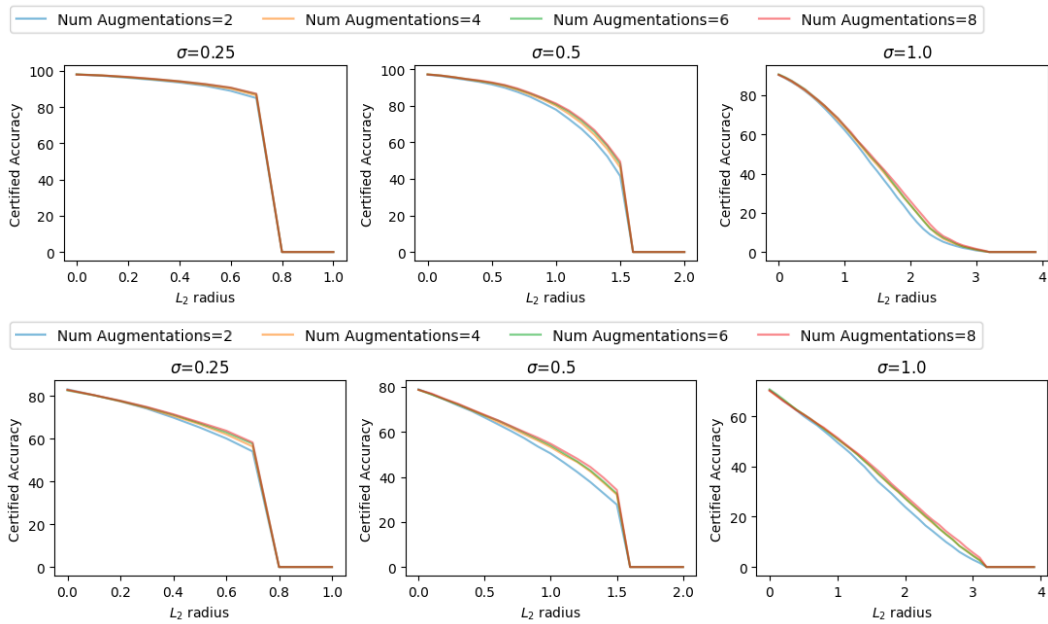


Figure 10: Certified accuracy comparison under different numbers of augmentations (2, 4, 6 and 8) on MNIST (top) and Fashion-MNIST (bottom)

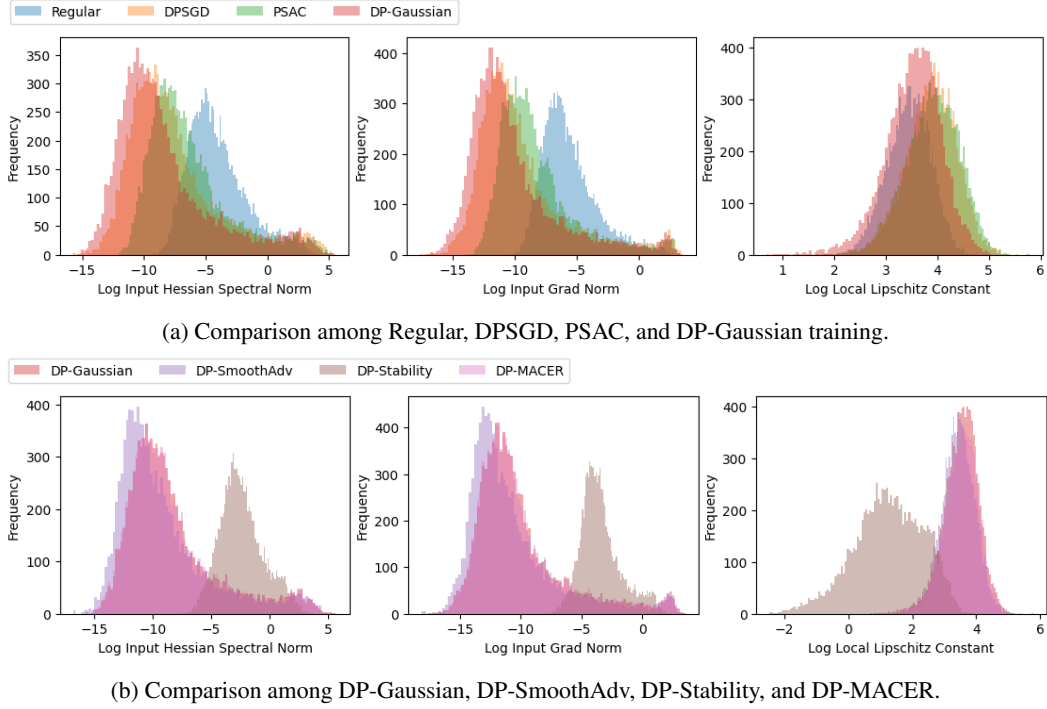
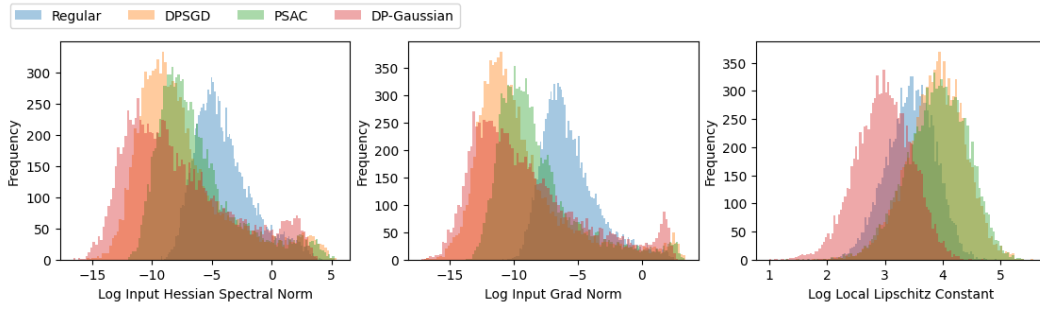


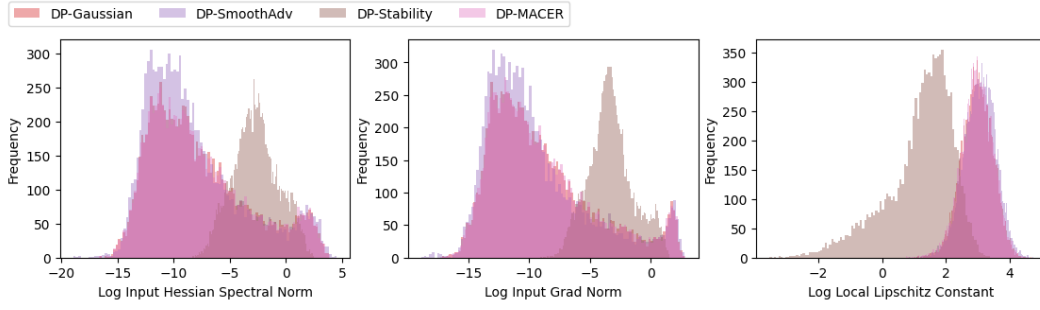
Figure 11: Per-sample metric comparisons on MNIST with $\sigma = 0.25$

D.3 Additional Per-sample Metric Analysis

Figures 11 through 15 show the distributions of our three proposed metrics for interpreting robustness, the input gradient norms, input Hessian spectral norms, and local Lipschitz constants. We use various training methods on MNIST and Fashion-MNIST under $\sigma \in \{0.25, 0.5, 1.0\}$. Echoing the analysis of RQ1 in Section 5.3, DPSGD produces a bimodal distribution for the Hessian and gradient norms, while Regular training exhibits a log-normal distribution and smaller tails for large metric values. PSAC shifts the distributions to be closer to those of Regular training by reducing clipping bias. DP-CERT methods, on the other hand, shift the distribution towards smaller metric values, resulting in higher certified accuracy. An exception is DP-Stability, which has significantly higher average gradient and Hessian norms, but without the mode at very high values, and with lower local Lipschitz constants than the other three variants.

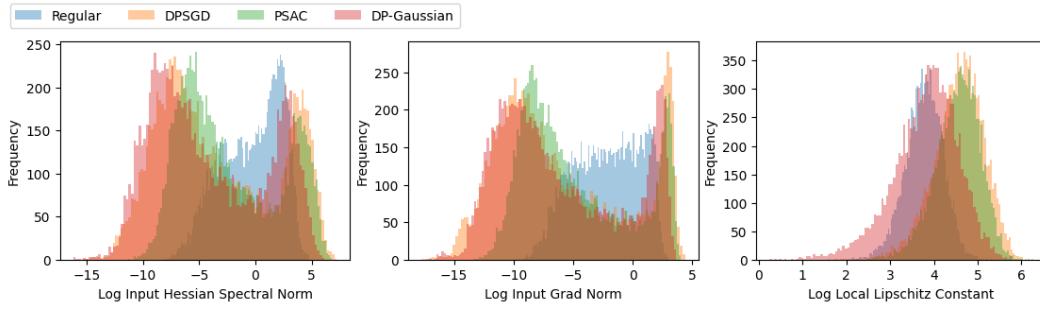


(a) Comparison among Regular, DPSGD, PSAC, and DP-Gaussian training.

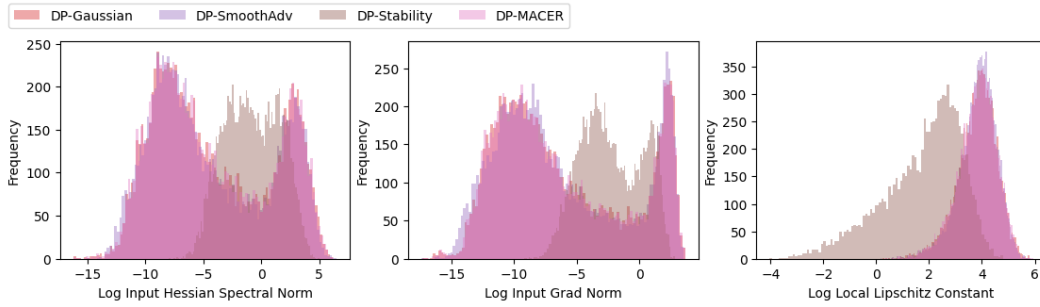


(b) Comparison among DP-Gaussian, DP-SmoothAdv, DP-Stability, and DP-MACER.

Figure 12: Per-sample metric comparisons on MNIST with $\sigma = 1.0$

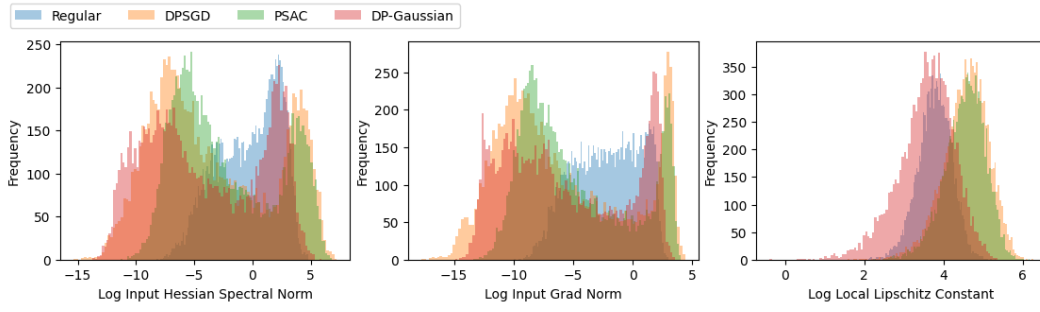


(a) Comparison among Regular, DPSGD, PSAC, and DP-Gaussian training.

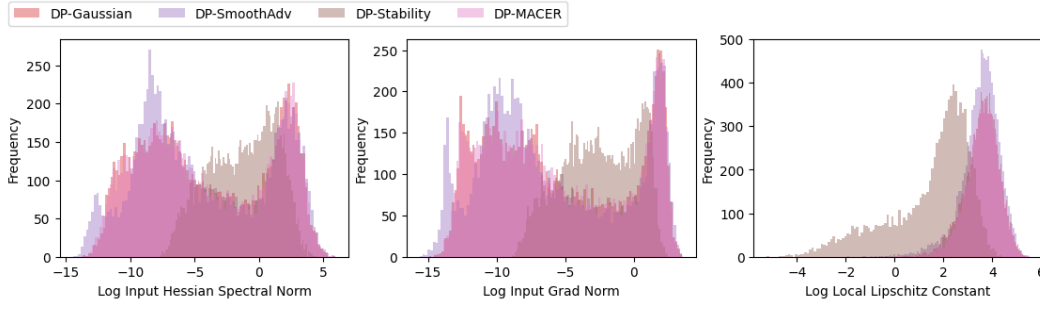


(b) Comparison among DP-Gaussian, DP-SmoothAdv, DP-Stability, and DP-MACER.

Figure 13: Per-sample metric comparisons on Fashion-MNIST with $\sigma = 0.25$

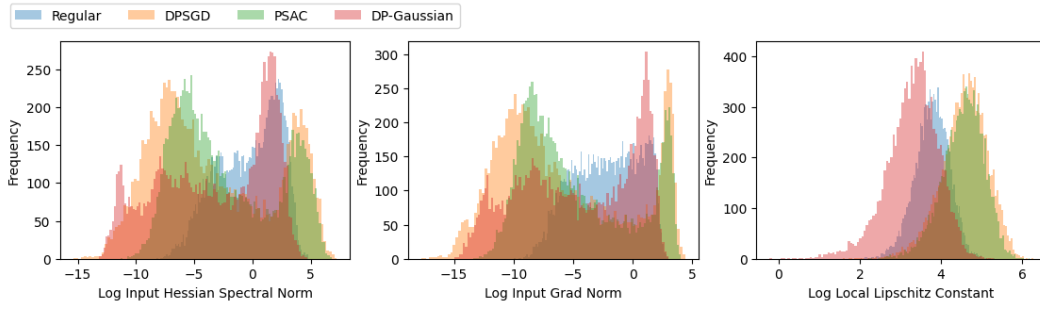


(a) Comparison among Regular, DPSGD, PSAC, and DP-Gaussian training.

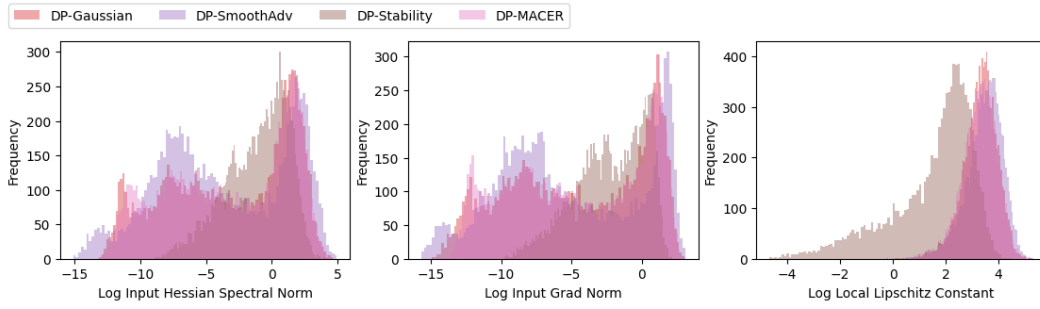


(b) Comparison among DP-Gaussian, DP-SmoothAdv, DP-Stability, and DP-MACER.

Figure 14: Per-sample metric comparisons on Fashion-MNIST with $\sigma = 0.5$



(a) Comparison among Regular, DPSGD, PSAC, and DP-Gaussian training.



(b) Comparison among DP-Gaussian, DP-SmoothAdv, DP-Stability, and DP-MACER.

Figure 15: Per-sample metric comparisons on Fashion-MNIST with $\sigma = 1.0$

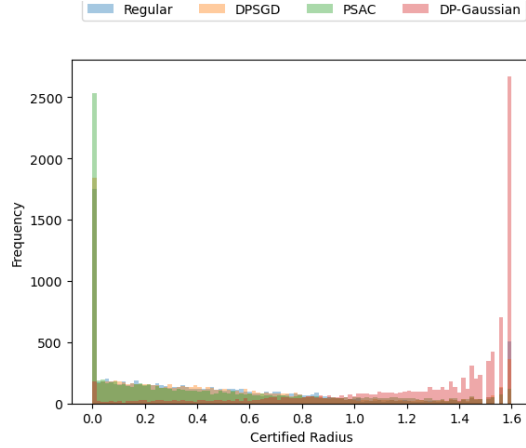


Figure 16: Distributions of certified radii for Regular, DPSGD, PSAC, and DP-Gaussian training on MNIST with $\sigma = 0.5$.

Figure 16 shows the distribution of certified radii for baseline training methods and an instance of DP-CERT for the same settings as Figure 4. Whereas Regular, DPSGD, and PSAC training all have a large spike of samples that cannot be certified at any level, DP-Gaussian achieves certified radii above 1.0 for most samples, with the mode even higher at 1.6.

While our main focus has been on certified robustness, we briefly compare to adversarial robustness against common attacks. Figure 17 shows the adversarial accuracy under a l_∞ -FGSM attack, with the attack strength in $\{0.0005, 0.01, 0.1, 0.5, 1\}$. Consistent with the ranking of the average local Lipschitz constant from Figures 11 through 15, DP-Stability consistently outperforms other approaches, while DP-Gaussian, DP-SmoothAdv, and DP-MACER all achieve similar adversarial accuracy above that of the unprotected baselines.

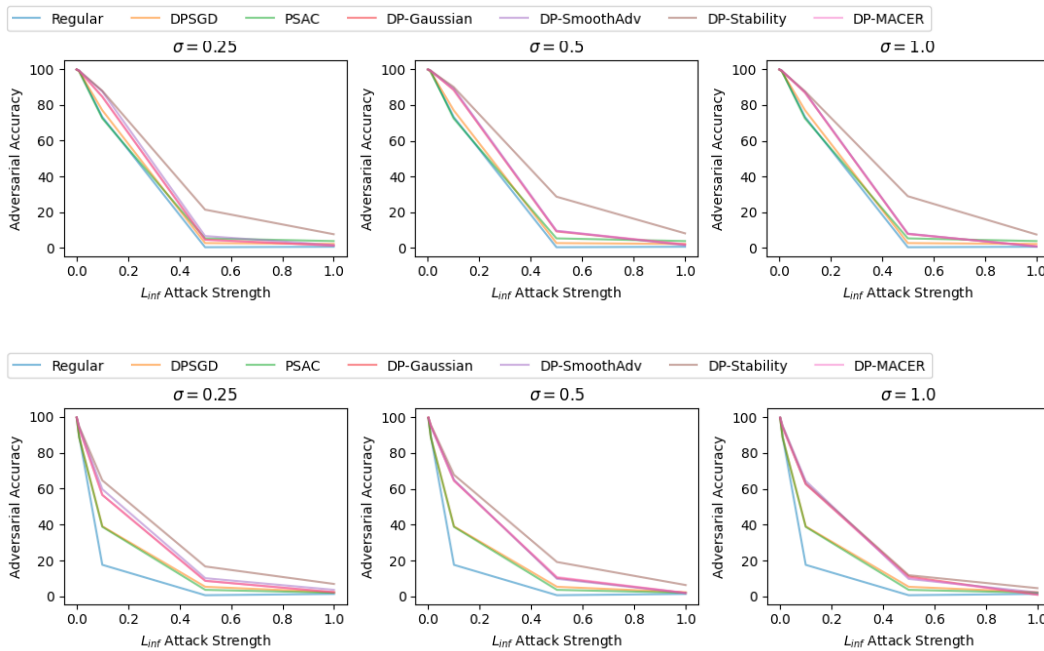
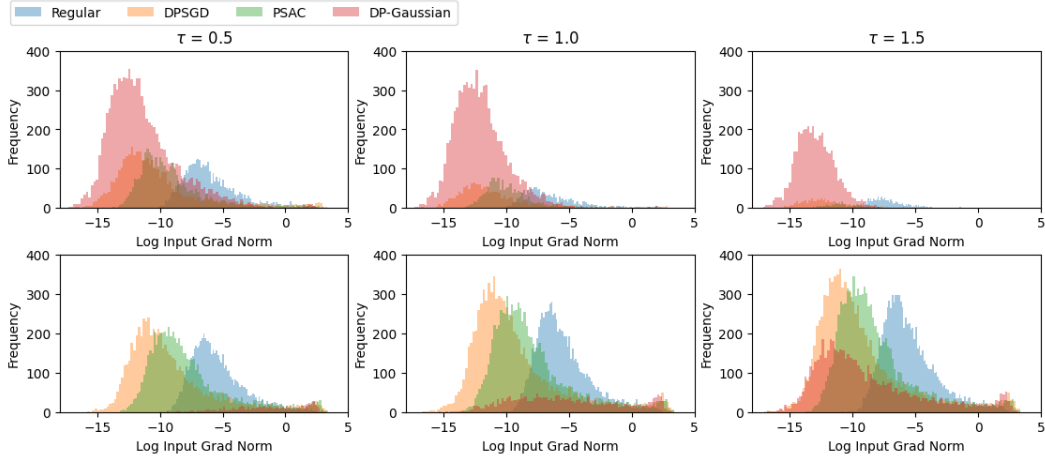
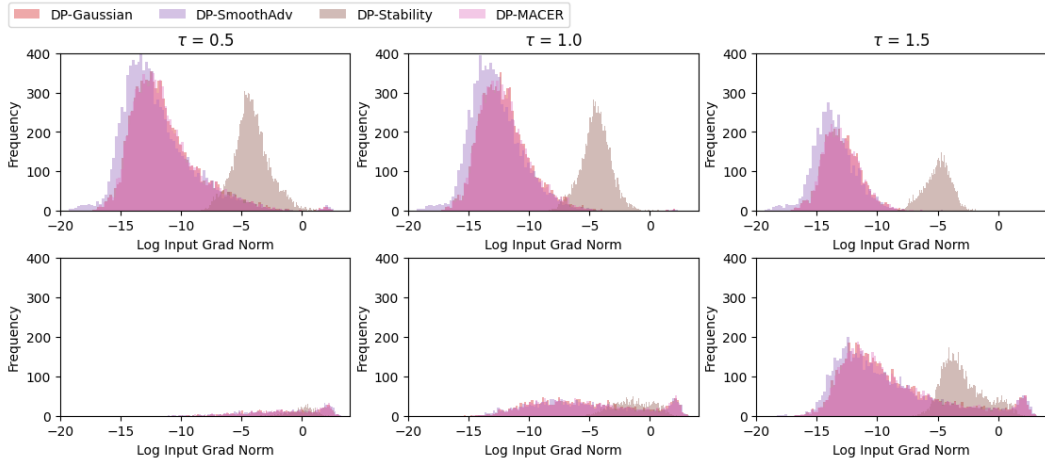


Figure 17: Adversarial accuracy against a L_∞ -FGSM attack under various attack strengths on MNIST (top) and Fashion-MNIST (bottom).



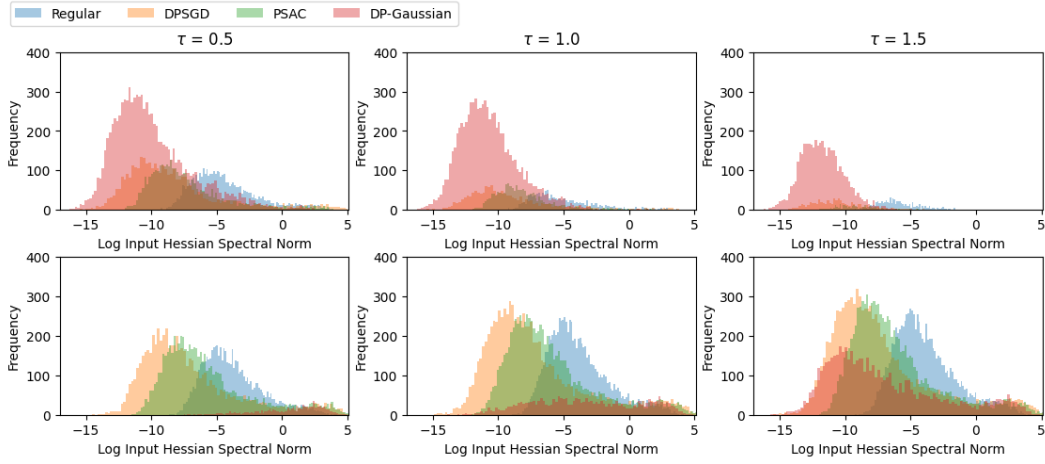
(a) Per-sample metric comparison among Regular, DPSGD, PSAC, and DP-Gaussian training.



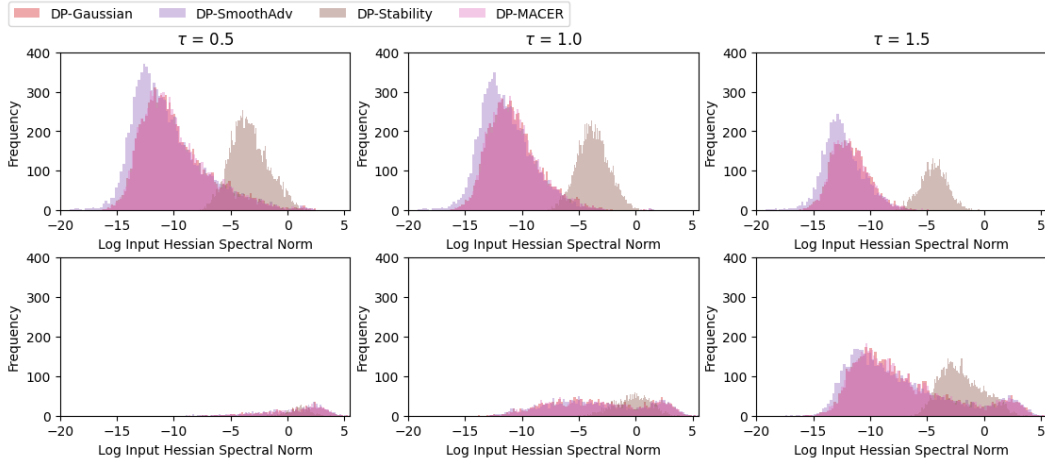
(b) Per-sample metric comparison among DP-Gaussian, DP-SmoothAdv, DP-Stability, and DP-MACER.

Figure 18: Comparing the distribution of *input gradient norm* of baselines and proposed methods on MNIST. All DP-CERT methods are trained with $\sigma = 0.5$. We show the logarithmic metric values for all methods for better visualization.

Finally, we study the metric distributions for individual samples that can or cannot be certified above a threshold τ , similar to Figure 6 in the main text. Figures 18 and 19 respectively show the input gradient norm and input Hessian spectral norm distributions for the baselines and proposed methods, with different threshold values $\tau \in \{0.25, 0.5, 1.0\}$. In each subfigure the top row shows samples that can be certified at radius larger than τ , and the bottom row shows samples that cannot. We only show the plots for MNIST under $\sigma = 0.5$ for brevity. We note that the shapes of the distributions between gradients and Hessians resemble each other closely. The analysis of RQ2 in Section 5.3 also applies here; for example, in Figure 18, the samples with certified radii below the threshold have slightly higher average input gradient norm. As the threshold τ increases, more examples with *higher* input gradient norm end up below the certified radius threshold. We find that the samples on which the models are least robust tend to be samples where the gradient and Hessian norms are largest. From this observation we expect that training methods that reduce the prevalence of large gradient and Hessian norms should be the most robust, which is indeed confirmed by DP-Stability which does not have the mode at very large values in Figures 11 through 15, and the best adversarial robustness in Figure 17.



(a) Per-sample metric comparison among Regular, DPSGD, PSAC, and DP-Gaussian training.



(b) Per-sample metric comparison among DP-Gaussian, DP-SmoothAdv, DP-Stability, and DP-MACER.

Figure 19: Comparing the distribution of *input Hessian spectral norm* of baselines and proposed methods on MNIST. All DP-CERT methods are trained with $\sigma = 0.5$. We show the logarithmic metric values for all methods for better visualization.